

# Plasticity-improved Zr–Cu–Al bulk metallic glass matrix composites containing martensite phase

Y. F. Sun

Research Center for Materials, Department of Materials Science and Engineering, Zhengzhou University, Zhengzhou 450002, People's Republic of China

B. C. Wei, Y. R. Wang, and W. H. Li

National Microgravity Lab, Institute of Mechanics, Chinese Academy of Sciences, Beijing 100080, People's Republic of China

T. L. Cheung and C. H. Shek<sup>a)</sup>

Department of Physics and Materials Science, City University of Hong Kong, Hong Kong, People's Republic of China

(Received 24 November 2004; accepted 16 June 2005; published online 25 July 2005)

Zr<sub>48.5</sub>Cu<sub>46.5</sub>Al<sub>5</sub> bulk metallic glass matrix composites with diameters of 3 and 4 mm were produced through water-cooled copper mold casting. Micrometer-sized bcc based B2 structured CuZr phase containing martensite plate, together with some densely distributed nanocrystalline Cu<sub>2</sub>Zr and plate-like Cu<sub>10</sub>Zr<sub>7</sub> compound, was found embedded in a glassy matrix. The microstructure formation strongly depends on the composition and cooling rate. Room temperature compression tests reveal significant strain hardening and plastic strains of 7.7% and 6.4% before failure are obtained for the 3-mm- and 4-mm-diam samples, respectively. The formation of the martensite phase is proposed to contribute to the strain hardening and plastic deformation of the materials.

© 2005 American Institute of Physics. [DOI: 10.1063/1.2006218]

Bulk metallic glasses (BMGs) have long been regarded as a potential structural material since their first emergence some 40 years ago. However, monolithic BMGs usually exhibit no yielding and strain hardening during room temperature deformation due to highly localized shear bands, which significantly limits the range of possible applications.<sup>1–6</sup> The attempt to improve the ductility of the BMG leads the development of BMG based composites.<sup>7</sup> In these composites, the second phase hinders single shear band to extend critically through the whole sample at the onset of plastic deformation and seeds the initiation of multiple shear bands. Therefore, plasticity is distributed more homogeneously in the shear band patterns, which results in high strains to failure of the composites.<sup>8–11</sup> Among the different bulk metallic glass composites, composites prepared by precipitation of ductile micrometer-sized particles upon cooling from the melt seem to be the most promising because dislocation motion, twinning or phase transformation induced plasticity are expected in the ductile phases.<sup>12,13</sup> Recently, ductile dendrite of bcc  $\beta$ -Ti phase, which significantly improves the deformation behavior of the composite compared to the monolithic glass, has been *in situ* formed in some Zr- or Ti-based multi-component BMGs with refractory element (Nb or Ta).<sup>14–18</sup> Martensite phases, which can generate numerous defects via phase transformation, have been used as reinforcement in many fields to improve the ductility or toughness of the materials, such as austenitic steel and ceramics, etc. However, no BMG matrix composites containing martensite phase have been reported so far.

In this letter we report Zr–Cu–Al ternary BMG matrix composite materials, which form a microstructure with the coexistence of CuZr compound containing martensite plate,

fine distributed particles and amorphous phase. The composites not only show high yield strength, but also exhibit significant strain hardening and plastic deformation before failure under uniaxial compression at room temperature.

An ingot of nominal composition Zr<sub>48.5</sub>Cu<sub>46.5</sub>Al<sub>5</sub> was prepared by arc melting under a Ti-gettered argon atmosphere. From this master alloy, bulk alloy rods with 3 and 4 mm diameters and 70 mm length were prepared by suction casting into a water-cooled copper mold in a purified argon atmosphere. The thermal stability was examined by differential scanning calorimetry (DSC) with a heating rate of 20 K min<sup>-1</sup> in a flowing argon atmosphere. The structures of the as-prepared alloys were analyzed by scanning electron microscopy (SEM) and transmission electron microscopy (TEM). Room temperature compression tests were carried out with an Instron 5562 testing machine under quasistatic loading (initial strain rate of 1 × 10<sup>-4</sup> s<sup>-1</sup>).

Figure 1 shows the x-ray diffraction (XRD) pattern re-

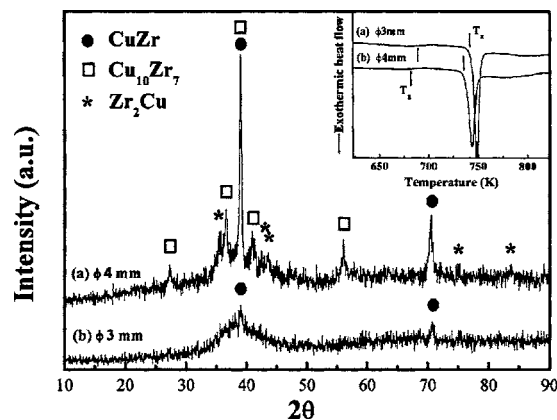


FIG. 1. XRD patterns of the as-cast rods inset with DSC scans at the constant heating rate of 20 K/min.

<sup>a)</sup> Author to whom correspondence should be addressed; electronic mail: apchshek@cityu.edu.hk

corded from the cross section of the as-cast alloys. For the 3-mm-diam sample, two small crystalline diffraction peaks superimposed on the broad amorphous diffraction peak were identified as CuZr phase. Apart from CuZr phase, more diffraction peaks identified as  $\text{Cu}_{10}\text{Zr}_7$  and  $\text{Zr}_2\text{Cu}$  were found for the 4-mm-diam sample. For DSC measurements, thin disk samples with weight of about 20 mg were cut from the alloy rods. The DSC profiles of the two samples inset in Fig. 1 all exhibit an obvious glass transition  $T_g$  followed by one exothermic reaction with onset temperature  $T_x$ . The  $T_g$  and  $T_x$  for samples with diameters of 3 and 4 mm are 689, 741 K and 683, 734 K, respectively. From the DSC curve, the heat of crystallization of the 3-mm-diam sample is higher than that of the 4-mm-diam sample. This reveals that the volume fraction of the crystals of the 4-mm-diam sample is higher than that of the 3-mm-diam sample.

SEM observations of each sample reveal that there exists an obvious microstructure transition from the center region to the edge due to different cooling rate. It can be observed that no crystals can be found on the homogeneous amorphous matrix in the outer part of the sample, while blocky grains with the size ranging from 20 to 60  $\mu\text{m}$  can be found near the center part. The grains display an uneven surface and contain plates with different lengths inside, which is shown in Fig. 2(a). The plates are self-arranged and align in different subcrystalline regions. The surface morphology of the grains reveals that a martensite phase might form during the rapid cooling of the alloy melts.

Further TEM analysis confirms the formation of martensite phase in CuZr compound, together with densely distributed nanocrystalline  $\text{Zr}_2\text{Cu}$  and plate-like  $\text{Cu}_{10}\text{Zr}_7$  phase. Figure 2(b) shows the CuZr parent phase and the martensite plate. The selected area electron diffraction (SAED) pattern taken along the [001] zone axial indicated that the CuZr parent phase has a bcc based B2 structure, with the lattice constant of  $a=3.256 \text{ \AA}$ . Moreover, regular weak diffraction spots can be observed on the SAED pattern, indicating that the CuZr phase is an ordered intermetallic and might have a superlattice atomic configuration. Previous studies of the microstructure of the martensite phase in CuZr have pointed out that it has a monoclinic symmetry and numerous two-dimensional defects crossing micro- as well as macrotwins which can be observed in all samples, regardless of the preparation technique used.<sup>19,20</sup> The atomic configuration of the martensite phase is complex and has been investigated in detail.<sup>21,22</sup> Figure 2(c) shows the densely formed microtwins of the martensite phase, which also is said to have some characterization of shape memory effect.<sup>21,22</sup> Figure 2(d) shows the uniformly distributed fine particles embedded in the glassy matrix. The particles can be assumed to be a mixture of nanocrystalline  $\text{Zr}_2\text{Cu}$  and plate-like  $\text{Cu}_{10}\text{Zr}_7$  according to the SAED pattern inset.<sup>23</sup> For the 3-mm-diam sample, nanocrystalline  $\text{Zr}_2\text{Cu}$  phase and plate-like  $\text{Cu}_{10}\text{Zr}_7$  can also be found, but its volume fraction is relatively smaller.

The different microstructures developed in different regions of the samples suggest that the solidification of the melt occurs in several steps. The melt in the outermost region of cylinder first freezes into an amorphous phase because of the high enough cooling rate near the mold. For a lower cooling rate towards the center of the sample, the CuZr phase precipitates and martensite phase transformation occurs with a high rate due to some kinetic effect. Upon formation of the CuZr phase, the residual melt was depleted of

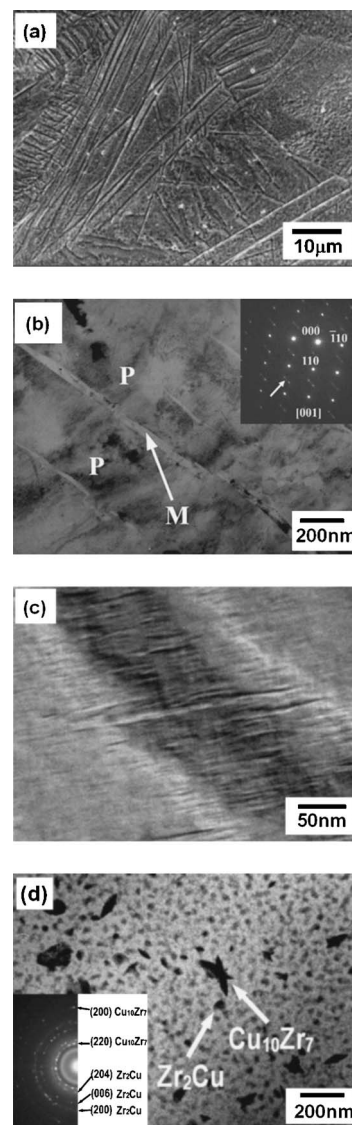


FIG. 2. Microstructure characterization of the as-cast 4-mm-diam alloy rod as typical example. (a) SEM image showing the macroscopic morphology of the martensite structure; TEM image showing (b) parent phase (“P”) and martensite phase (“M”) with SAED pattern inside; (c) densely formed microtwins in the martensite plate; and (d) fine particles distributed in glassy matrix.

Cu and Zr and becomes enriched in Al towards a concentration where the solidification of the residual melt into a glass is favored.<sup>24</sup> However, the CuZr phase is a metastable phase below 985 K. Some CuZr crystals in the region with slow cooling rate will decompose into  $\text{Cu}_{10}\text{Zr}_7$  and  $\text{Zr}_2\text{Cu}$  phases during the solidification of residual melts.<sup>25</sup>

Room temperature compression tests reveal that the *in situ* composites undergo obvious strain hardening and plastic deformation prior to failure. Typical examples of the compressive stress-strain curves for the 3-mm- and 4-mm-diam samples are shown in Fig. 3. The curve for the 3-mm-diam sample has been displaced for clarity. For the 3-mm-diam sample, the sample showed an ultimate compressive strength of 1894 MPa, a yield strength of 1332 MPa, and plastic deformation of 7.7%. For the 4-mm-diam sample, the sample showed an ultimate compressive strength of 1910 MPa, a yield strength of 1624 MPa, and plastic deformation of 6.4%.

The compression tests confirm that the  $\text{Zr}_{48.5}\text{Cu}_{46.5}\text{Al}_5$  composites still deform by the formation and propagation of

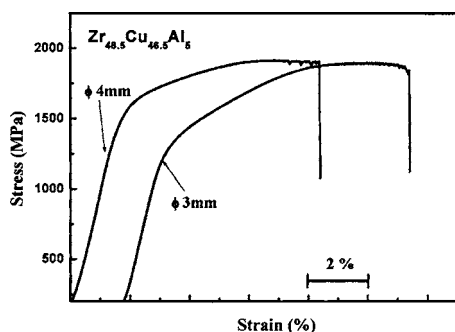


FIG. 3. Compressive strain and stress curves of  $Zr_{48.5}Cu_{46.5}Al_5$  alloys with diameter of 3 and 4 mm.

multiple shear bands in the shear plane, which is inclined at an angle of about  $45^\circ$  to the loading direction. Figure 4 shows the fracture morphology of the center region for the 4-mm-diam sample; after a compression test, the grains are elongated vertical to the loading direction. It was generally believed that the nanocrystals embedded in an amorphous matrix can only provide high strength, but not strain hardening owing to the lack of substantial dislocations multiplication, while the amorphous phase only process strain softening upon loading. In the present condition, the micrometer-sized CuZr phase might experience strain hardening and act as an obstacle to the local shear deformation, thus retarding the shear fracture of the alloy. As a result, the materials exhibit high strength and large plastic strain at the same time. One of the factors that promoted the strain hardening, we believe, is the twinning deformation in the CuZr grains.

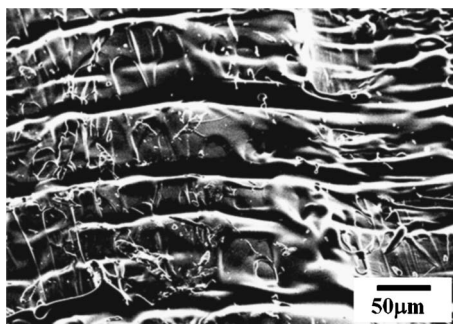


FIG. 4. SEM image showing the fracture morphology of the center region for 4-mm-diam sample after room temperature compression test.

In conclusion, the  $Zr_{48.5}Cu_{46.5}Al_5$  BMG composites containing martensite phase can be formed. The formation of this microstructure is strongly governed by the alloy composition and the cooling rate of solidification. The mechanical strength and plastic deformation of the materials increase distinctly due to the presence of the martensite phase.

The authors are grateful to Professor W. H. Wang from the Institute of Physics, CAS, for stimulating discussions. This work was supported by a City University of Hong Kong Strategic Research Grant (Project No. 7001529) and National Nature Science Foundation of China (Grant No. 50101012).

- <sup>1</sup>D. V. Louzguine, H. Kato, and A. Inoue, *Appl. Phys. Lett.* **84**, 1088 (2004).
- <sup>2</sup>A. Inoue, *Mater. Trans., JIM* **36**, 866 (1995).
- <sup>3</sup>A. Inoue, *Acta Mater.* **48**, 279 (2000).
- <sup>4</sup>L. Q. Xing, Y. Li, K. T. Ramesh, J. Li, and T. C. Hufnagel, *Phys. Rev. B* **64**, 180201 (2001).
- <sup>5</sup>H. Choi-Yim, R. Busch, U. Koster, and W. L. Johnson, *Acta Mater.* **47**, 2455 (1999).
- <sup>6</sup>C. A. Pampillo, *J. Mater. Sci.* **10**, 1194 (1975).
- <sup>7</sup>H. Choi-Yim and W. L. Johnson, *Appl. Phys. Lett.* **71**, 3808 (1997).
- <sup>8</sup>H. Choi-Yim, R. Busch, U. Koster, and W. L. Johnson, *Acta Mater.* **47**, 2455 (1999).
- <sup>9</sup>H. Ma, J. Xu, and E. Ma, *Appl. Phys. Lett.* **83**, 2793 (2003).
- <sup>10</sup>C. P. Kim, R. Busch, A. Masuhr, H. Choi-Yim, and W. L. Johnson, *Appl. Phys. Lett.* **79**, 1456 (2001).
- <sup>11</sup>A. Leonhard, L. Q. Xing, M. Heilmair, A. Gebert, J. Eckert, and L. Schultz, *Nanostruct. Mater.* **10**, 805 (1998).
- <sup>12</sup>J. Eckert, U. Kuhn, N. Mattern, G. He, and A. Gebert, *Inzh.-Fiz. Zh.* **10**, 1183 (2002).
- <sup>13</sup>E. Ma, *Nat. Mater.* **2**, 7 (2002).
- <sup>14</sup>U. Kuhn, J. Eckert, N. Mattern, and L. Schultz, *Appl. Phys. Lett.* **80**, 2478 (2002).
- <sup>15</sup>C. C. Hays, C. P. Kim, and W. L. Johnson, *Phys. Rev. Lett.* **84**, 2901 (2000).
- <sup>16</sup>G. He, J. Eckert, W. Loser, and L. Schultz, *Nat. Mater.* **2**, 33 (2003).
- <sup>17</sup>U. Kuhn, J. Eckert, N. Mattern, and L. Schultz, *Mater. Sci. Eng., A* **375-377**, 322 (2004).
- <sup>18</sup>F. Szuets, C. P. Kim, and W. J. Johnson, *Acta Mater.* **49**, 1507 (2001).
- <sup>19</sup>A. W. Nicholls and I. R. Harris, *J. Mater. Sci. Lett.* **5**, 217 (1986).
- <sup>20</sup>E. M. Carvalho and I. R. Harris, *J. Mater. Sci.* **15**, 1224 (1980).
- <sup>21</sup>J. W. Seo and D. Schryvers, *Acta Mater.* **46**, 1165 (1998).
- <sup>22</sup>J. W. Seo and D. Schryvers, *Acta Mater.* **46**, 1177 (1998).
- <sup>23</sup>H. R. Wang, Y. F. Ye, and Z. Q. Shi, *J. Non-Cryst. Solids* **36**, 311 (2002).
- <sup>24</sup>Y. Yokoyama, A. Kobayashi, K. Fukaura, and A. Inoue, *Mater. Trans., JIM* **43**, 571 (2002).
- <sup>25</sup>L. Q. Xing and P. Ochin, *Acta Mater.* **45**, 3765 (1997).